Human Molecular Genetics, 2012, Vol. 21, No. 4 **841–851**
doi:10.1093/hmg/ddr514
Advance Access published on November 9, 2011

A novel tyrosine kinase inhibitor restores chondrocyte differentiation and promotes bone growth in a gain-of-function Fgfr3 mouse model

Aurélie Jonquoy[1], Emilie Mugniery[1], Catherine Benoist-Lasselin[1], Nabil Kaci[1], Laurent Le Corre[2], Florent Barbault[3], Anne-Lise Girard[2], Yves Le Merrer[2], Patricia Busca[2], Laurent Schibler[4], Arnold Munnich[1] and Laurence Legeai-Mallet[1,*]

[1]INSERM U781-Université Paris Descartes-Hôpital Necker-Enfants Malades, Paris 75015, France, [2]Université Paris Descartes-CNRS UMR 8601, Laboratoire de Chimie et Biochimie Pharmacologiques et Toxicologiques, Paris 75006, France, [3]Université Paris Diderot-Laboratoire ITODYS, Paris 75013, France and [4]UMR1313 Génétique Animale et Biologie Intégrative, INRA, Jouy-en-Josas 78350, France

Received September 13, 2011; Revised September 13, 2011; Accepted November 1, 2011

Activating germline fibroblast growth factor receptor 3 (FGFR3) mutations cause achondroplasia (ACH), the most common form of human dwarfism and a spectrum of skeletal dysplasias. FGFR3 is a tyrosine kinase receptor and constitutive FGFR3 activation impairs endochondral ossification and triggers severe disorganization of the cartilage with shortening of long bones. To decipher the role of FGFR3 in endochondral ossification, we analyzed the impact of a novel tyrosine kinase inhibitor (TKI), A31, on both human and mouse mutant FGFR3-expressing cells and on the skeleton of *Fgfr3*$^{Y367C/+}$ dwarf mice. We found that A31 inhibited constitutive FGFR3 phosphorylation and restored the size of embryonic dwarf femurs using an *ex vivo* culture system. The increase in length of the treated mutant femurs was 2.6 times more than for the wild-type. Premature cell cycle exit and defective chondrocyte differentiation were observed in the *Fgfr3*$^{Y367C/+}$ growth plate. A31 restored normal expression of cell cycle regulators (proliferating cell nuclear antigen, KI67, cyclin D1 and p57) and allowed pre-hypertrophic chondrocytes to properly differentiate into hypertrophic chondocytes. Our data reveal a specific role for FGFR3 in the cell cycle and chondrocyte differentiation and support the development of TKIs for the treatment of FGFR3-related chondrodysplasias.

INTRODUCTION

Skeletal development in humans is regulated by numerous growth factors. Among them fibroblast growth factor receptor 3 (FGFR3), a tyrosine kinase receptor, has been described as both a negative and a positive regulator of endochondral ossification (1–4). Gain-of-function mutations of FGFR3 disrupt endochondral ossification in a spectrum of skeletal dysplasias which include ACH, the most common form of human dwarfism (5,6), hypochondroplasia (7,8) and thanatophoric dysplasia (TD) (9–11) and in *Fgfr3* mouse models (12–15). Activated FGFR3 reduces the rate of cartilage template formation and disrupts chondrocyte proliferation and differentiation, leading to a severe disorganization of the growth plate cartilage. FGFR3-related chondrodysplasias are the result of increased signal transduction from the activated receptor.

Several signaling pathways have been described downstream of FGFR3 activation, including the extracellular signal-regulated kinases (ERK) and p38 mitogen-activated protein kinase (MAPK) pathways (16–19) and the signal transducer and activation of transcription pathway (20–22). Others pathways such as the phosphoinositide 3 kinase-AKT (23) and protein kinase C pathways in endochondral bone growth have been identified. The degradation of mutant receptors is disturbed as demonstrated by higher levels of FGFR3 mutant receptors at the cell surface (24–26) and disruption of c-Cbl-mediated ubiquitination (27). Fgfr3 mutations disrupt the formation of glycosylated isoforms of the receptor and impeded its trafficking (28,29).

*To whom correspondence should be addressed. Tel: +33 144494000; Fax: +33 147348514; Email: laurence.legeai-mallet@inserm.fr

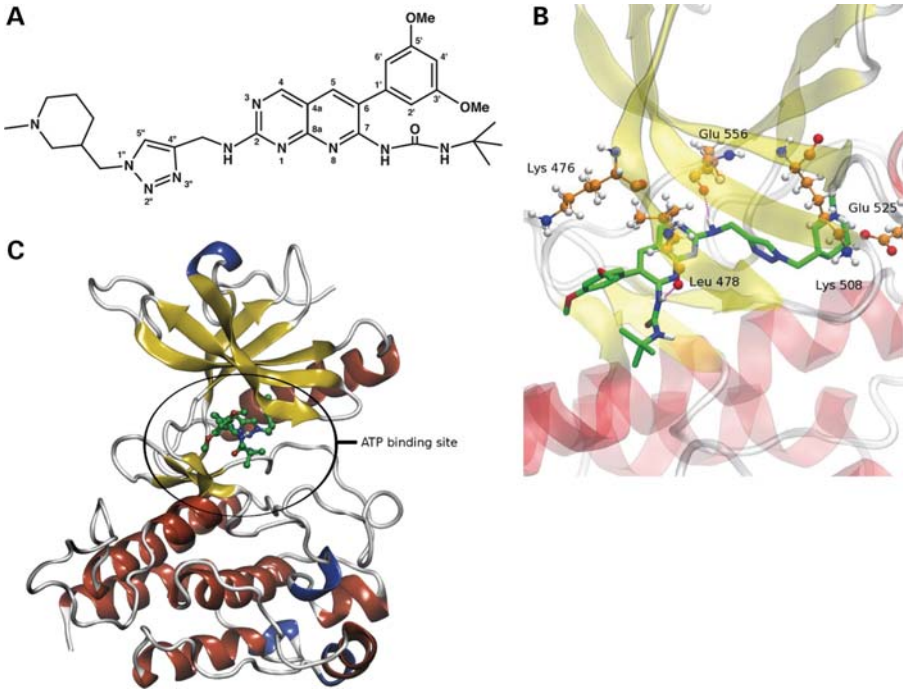

Figure 1. A31 prevents the kinase activity of FGFR3. (**A**) Molecular scheme of the A31 compound. (**B**) Overall structure showing docking conformation of A31 inside the FGFR3-binding pocket. A31 is represented with colored rods (carbon in green, oxygen in red, nitrogen in blue and polar hydrogen in white). The FGFR3 kinase domain is shown as transparent ribbons and interacting amino acids in balls and rods with carbon in orange. (**C**) Overall structure showing A31 in the ATP-binding site.

To date, several strategies aimed at reducing excessive activation of FGFR3 have been proposed (30). They include strategies to inhibit FGFR3 tyrosine kinase activity, to promote its degradation and to antagonize its downstream signals (30). However, the mechanisms by which mutated FGFR3 disrupts bone growth are poorly understood. Here, to decipher the role of FGFR3 in the endochondral ossification process, we tested a synthetic compound of the pyrido-[2,3-*d*] pyrimidine class, A31 (31), as a novel tyrosine kinase inhibitor (TKI) which competes with the adenosine triphosphate (ATP)-binding site of FGFR3. We modeled its binding to the FGFR3 kinase domain *in silico*, with the disruption of kinase activity predicted by this analysis. We showed the ability of A31 to inhibit the constitutive phosphorylation of FGFR3 in human chondrocyte lines (32) transiently expressing activated forms of FGFR3 (28). To delineate the functional impact of FGFR3 mutation during cartilage development, we studied a gain-of-function *Fgfr3*$^{Y367C/+}$ mouse model (14) and showed that A31 restored the size of femurs isolated from *Fgfr3*$^{Y367C/+}$ murine embryos to wild-type (WT) length and increased the hypertrophic zone as revealed by type X collagen labeling.

Studying several cell cycle regulators (cyclin D1, p57) and markers of proliferation [proliferating cell nuclear antigen (PCNA), KI67], we observed an overexpression of these markers in *Fgfr3*$^{Y367C/+}$ growth plates. A31 strongly decreased the expression of these markers in the proliferative and hypertrophic zones. This TKI had a remarkable effect on bone growth and allowed pre-hypertrophic (PH) chondrocytes to differentiate into hypertrophic chondrocytes. These data allow us to conclude that activating *Fgfr3* mutations induce cell cycle exit and promote abnormal chondrocyte maturation. By targeting the FGFR3 kinase domains with A31 in *Fgfr3*$^{Y367C/+}$ mice, our results suggest that TKI holds promise for therapeutic approaches in FGFR3-related chondrodysplasias.

RESULTS

Strong interaction between the tyrosine kinase domain of FGFR3 and A31

Computational analyses were used to estimate interactions between FGFR3 and A31, a synthetic compound of the pyrido-[2,3-*d*] pyrimidine class, as a novel FGFR3 TKI (31) (Fig. 1A).

To date, attempts to determine the experimental X-ray structure of the FGFR3 kinase domain have failed. To overcome this drawback, we predicted the structure of FGFR3 *in silico* by using a new crystal structure of the highly homologous FGFR1 (33). The resulting 3D structure of FGFR3 showed a low global energy and negative electrostatic and Van der Waals components, indicating a high level of confidence for this prediction. Docking calculations were used to find the optimal position of A31 in the binding pocket of FGFR3. The interactions between the FGFR3 kinase domain and A31 are depicted in Figure 1B. The aromatic group carrying the two methoxy moieties and the biphenyl ring induce strong interactions between the FGFR3 kinase domain and A31. Two hydrogen bonds locate the biphenyl ring at the

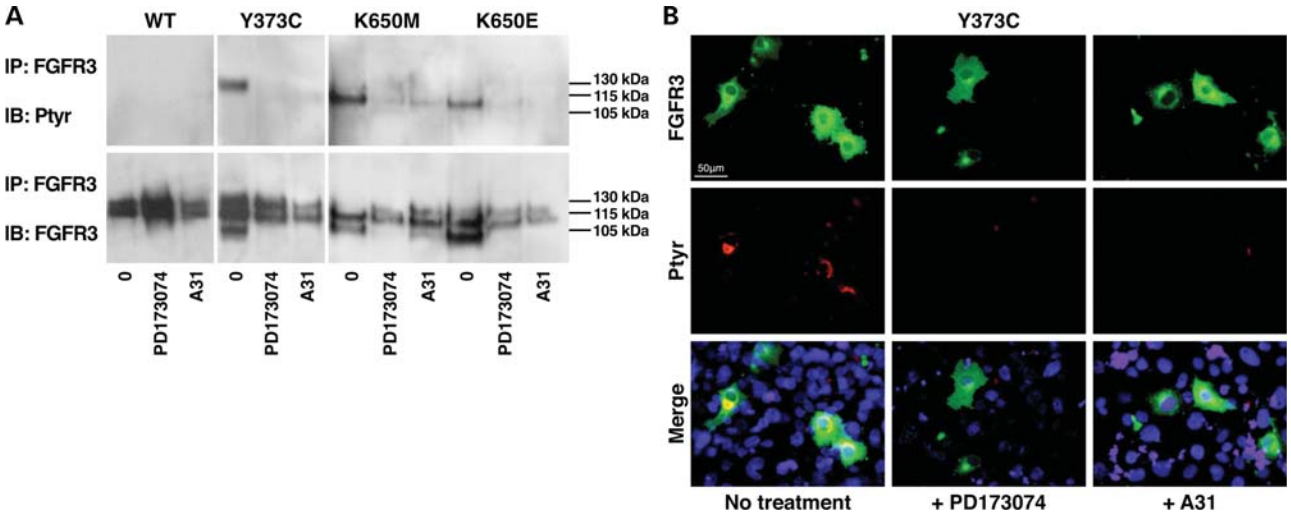

Figure 2. A31 inhibits the constitutive activation of FGFR3. (**A**) Immunoblots showing FGFR3 overexpression in transfected cells (HEK) with WT human-cDNA ($FGFR3^{+/+}$) and three human mutant cDNA constructs ($FGFR3^{Y373C}$, $FGFR3^{K650E}$, $FGFR3^{K650M}$). FGFR3 is immunoprecipitated (IP) and immunoblotted (IB) with anti-FGFR3 and anti-phosphotyrosine antibodies (Ptyr). Ptyr immunoblot showing constitutive phosphorylation of FGFR3 in transfected cells with mutant cDNA constructs. FGFR3 immunoblots showing three isoforms of the protein (105, 115 and 130 kDa) in WT ($FGFR3^{+/+}$) and one mutant ($FGFR3^{Y373C}$). Two isoforms of the FGFR3 protein (105 and 115 kDa) were present in cells transfected with mutant constructs ($FGFR3^{K650M}$ and $FGFR3^{K650E}$). A31 reduces the constitutive phosphorylation of FGFR3. (**B**) Immunocytochemistry showing FGFR3 (green), phosphorylated tyrosine proteins (red) and nucleus (blue, DAPI staining) in human chondrocytes transfected with mutant cDNA ($FGFR3^{Y373C}$). A31 abolishes constitutive FGFR3 phosphorylation in transfected cells. All experiments were performed in triplicate.

adenine position of ATP, filling the FGFR3 active site and, in this way, A31 competes directly with the substrate. The cyclic amino tail of A31 is deeply nestled inside the FGFR3 cavity in the vicinity of a protein salt bridge. As a consequence, the salt bridge is disrupted, thus preventing the kinase activity of FGFR3 (Supplementary Material, Fig. S1). These *in silico* data suggest that A31 specifically inhibits FGFR3 kinase activity.

A31 inhibits FGFR3 phosphorylation and proliferation of mutant Fgfr3 cell lines

Previously, we designed a library of pyrido[2,3-*d*]pyrimidines as the FGFR3 TKI. Among the 27 analogues synthesized, one TKI, A31, which exhibited 89% inhibition of FGFR3 kinase activity was selected (31). Here, we evaluated the ability of A31 to inhibit the constitutive phosphorylation of FGFR3 in human chondrocyte lines (28) transiently expressing activated forms of FGFR3 [$FGFR3^{Y373C}$ or $FGFR3^{K650E}$ (TD), $FGFR3^{K650M}$ (SADDAN) or $FGFR3^{+/+}$]. Immunoprecipitation and western blotting showed the presence of a 130 kDa mature isoform in the WT and $FGFR3^{Y373C}$ cell lysates, whereas only an 115 kDa immature form was present in $FGFR3^{K650M}$ and $FGFR3^{K650E}$ lysates (Fig. 2A). A31 abolished receptor phosphorylation in all cells expressing FGFR3 mutations (Fig. 2A). Similar results were found with a commercial TKI inhibitor (PD173074) (Fig. 2A). This inhibition was confirmed by immunocytochemistry in transfected cells expressing FGFR3 mutations (Fig. 2B). We observed a complete inhibition of FGFR3 phosphorylation by A31.

These data confirmed the ability of A31 to inhibit constitutive FGFR3 phosphorylation in transfected cells. To determine whether A31 modulates the mitogenic activity of activated FGFR3, we measured [3H]-thymidine incorporation in $FGFR3^{Y373C}$ and $FGFR3^{K650M}$ transfected NIH3T3 cells. The mitogenic activity was increased in cells expressing FGFR3 mutations compared with WT ($FGFR3^{Y373C}$, 9927 ± 2921 cpm; $FGFR3^{K650M}$, 15048 ± 5251 cpm; WT, 7499 ± 1667 cpm; $P < 10^{-5}$ versus WT) (Supplementary Material, Fig. S2).

A31 treatment strongly reduced DNA synthesis of all mutant cell lines [$FGFR3^{Y373C}$, 3144 ± 1201 cpm; $FGFR3^{K650M}$, 6281 ± 2699 cpm; $^{**}P < 10^{-10}$, $^{***}P < 10^{-20}$ versus dimethyl sulfoxide (DMSO)] (Supplementary Material, Fig. S2). These results demonstrate that A31 decreases the mitogenic activity of FGFR3 mutants.

Rescue of the $Fgfr3^{Y367C/+}$ femur growth defect by A31

A31 was tested on a gain-of-function $Fgfr3^{Y367C/+}$ mouse model (14). $Fgfr3^{Y367C/+}$ mice display reduced length of long bones, broad femurs, a narrow trunk, short ribs and a slightly dome-shaped skull, closely resembling ACH (Fig. 3A and B). We analyzed the effects of A31 on endochondral ossification in $Fgfr3^{Y367C/+}$ mice by using an *ex vivo* culture system for embryonic day 16.5 (E16.5) limb explants. Mutant femurs cultured without A31 had a significantly reduced longitudinal growth compared with WT ($Fgfr3^{Y367C/+}$, 461 ± 119 µm; WT, 1247 ± 226 µm; $P < 10^{-10}$) (Fig. 3C and D). A31 was able to induce and fully restore limb growth in $Fgfr3^{Y367C/+}$ femurs ($Fgfr3^{Y367C/+}$, gain of 1880 ± 558 µm; WT, 1863 ± 255 µm; $P < 10^{-19}$) (Fig. 3C and D). After 5 days of culture, the increase in length of the treated mutant femurs was 2.6 times more than that of WT.

Histological examinations using Hematoxylin-eosin (HES) staining (Fig. 4A) and type X collagen labeling (Fig. 4B)

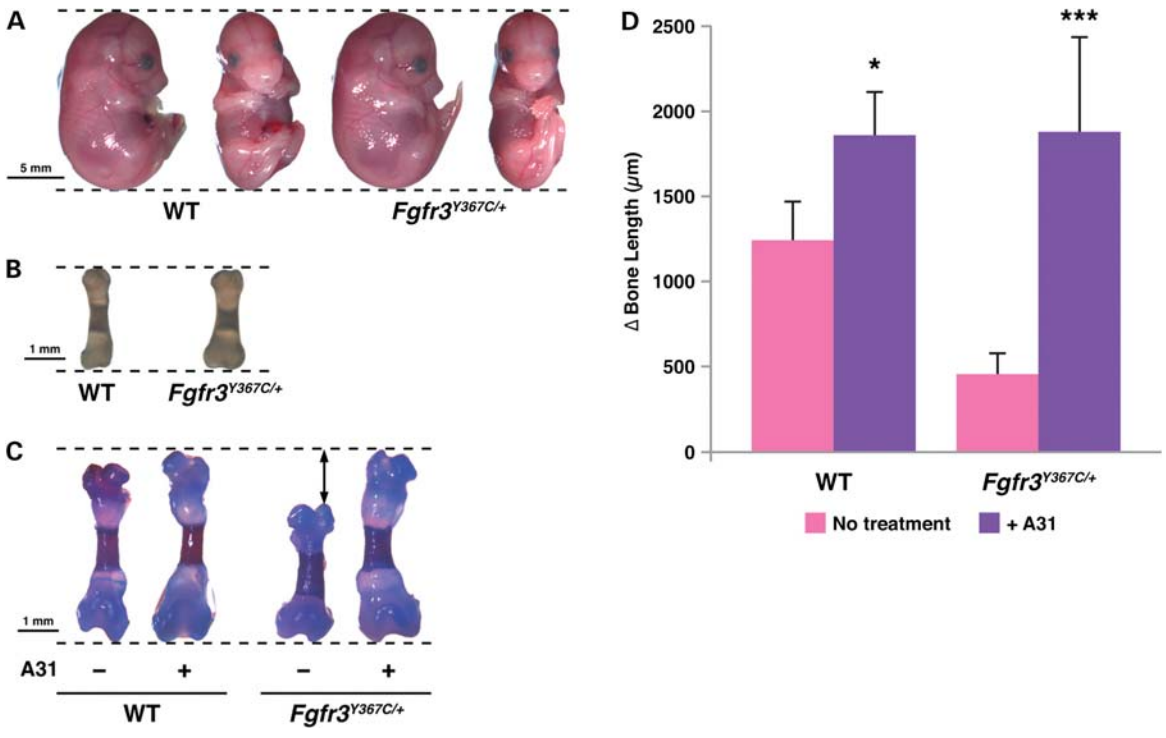

Figure 3. A31 restores longitudinal bone growth of *Fgfr3*$^{Y367C/+}$ femurs. (**A**) *Fgfr3*$^{Y367C/+}$ mouse embryo at E16.5 shows a dome-shape skull. (**B**) *Fgfr3*$^{Y367C/+}$ femur is broader with a shorter diaphysis at E16.5. (**C**) Alizarin red and Alcian blue staining show the small size of *Fgfr3*$^{Y367C/+}$ femurs. A31 increases the size of the *Fgfr3*$^{Y367C/+}$ femurs after 5 days of culture. (**D**) Bone length measurements showing a reduced longitudinal growth in *Fgfr3*$^{Y367C/+}$ femurs compared with WT (*Fgfr3*$^{Y367C/+}$, 461 ± 119 μm; WT, 1247 ± 227 μm; $P < 10^{-10}$). A31 enhances longitudinal growth in *Fgfr3*$^{Y367C/+}$ femurs, the bone growth is greater in *Fgfr3*$^{Y367C/+}$ femurs compared with controls (*Fgfr3*$^{Y367C/+}$, 1880 ± 558 μm; WT, 1863 ± 255 μm; $^{***}P < 10^{-19}$ versus untreated controls). The experiments were performed six times and bone length is shown as mean ± SD.

revealed a reduction in size of the hypertrophic zone of the *Fgfr3*$^{Y367C/+}$ mouse growth plate (Fig. 4B), with abnormally small chondrocytes resembling PH rather than hypertrophic cells (Fig. 4C). We evaluated the impact of A31 on the growth plate (Fig. 4A). Interestingly, A31 induced a marked expansion of the hypertrophic zone, with marked modifications of the shape of proliferative and hypertrophic cells. A31-treated chondrocytes appeared enlarged and more spherical, resembling to hypertrophic chondrocytes (Fig. 4D). Therefore, these results suggest that A31 increased the size of mutant growth plates by restoring the disrupted chondrocyte maturation process.

Effect of A31 on Fgfr3 protein expression

We evaluated the level of Fgfr3 protein expression by immunohistochemical staining and found an overexpression of Fgfr3 in *Fgfr3*$^{Y367C/+}$ growth plates (Fig. 5A). A31 induced a large decrease in Fgfr3 expression in mutant femurs (Fig. 5A). These results were confirmed by western blotting on primary chondrocytes isolated from E16.5 ribs (Fig. 5B). A higher level of Fgfr3 was revealed in untreated *Fgfr3*$^{Y367C/+}$ chondrocytes, whereas this level was similar to WT after addition of A31. These data, as previously suggested (26), confirm that the inhibition of the constitutive phosphorylation of Fgfr3 by A31 rescues the turnover of the receptor.

A31 modulates the expression of cell cycle regulator genes

Analysis of expression of PCNA, an S-phase marker, revealed abnormally high levels of PCNA in the PH (73% of total cells positive; $P < 0\,005$) and hypertrophic (H) areas of *Fgfr3*$^{Y367C/+}$ mouse growth plates (43% of total cells positive; $P <$ 0,005) (Fig. 6A). A31 strongly decreased PCNA expression in the corresponding areas of mutant growth plates (20 and 18% for PH and H areas, respectively, $^{***}P < 10^{-4}$) (Fig. 6B). Likewise, higher expression levels of KI67 were observed in the PH and H areas of *Fgfr3*$^{Y367C/+}$ mouse growth plates compared with controls (Fig. 6C). A31 also decreased this expression in *Fgfr3*$^{Y367C/+}$ mouse growth plates (Fig. 6C). We noted a higher expression of PCNA than KI67 in the mutant growth plate. Furthermore, we investigated whether the presence of mutated Fgfr3 caused an impairment of expression of cell cycle regulators. In fact, activated *Fgfr3* induced a significant overexpression of cyclin D1 in the proliferative and PH chondrocytes of *Fgfr3*$^{Y367C/+}$ mice (Fig. 6D). Interestingly, A31 returned cyclin D1 expression to control levels in mutant femurs (Fig. 6D). Consistent with this, western blots showed a reduced level of cyclin D1 in A31-treated murine chondrocytes isolated from E16.5 ribs compared with untreated chondrocytes (Fig. 6F). We further analyzed the level of cyclin-dependent kinase (CDK) inhibitors (CDKIs) negatively regulating the cell cycle (34), particularly p57, a member of the Cip/Kip family (35). Activated Fgfr3 induced a higher expression of

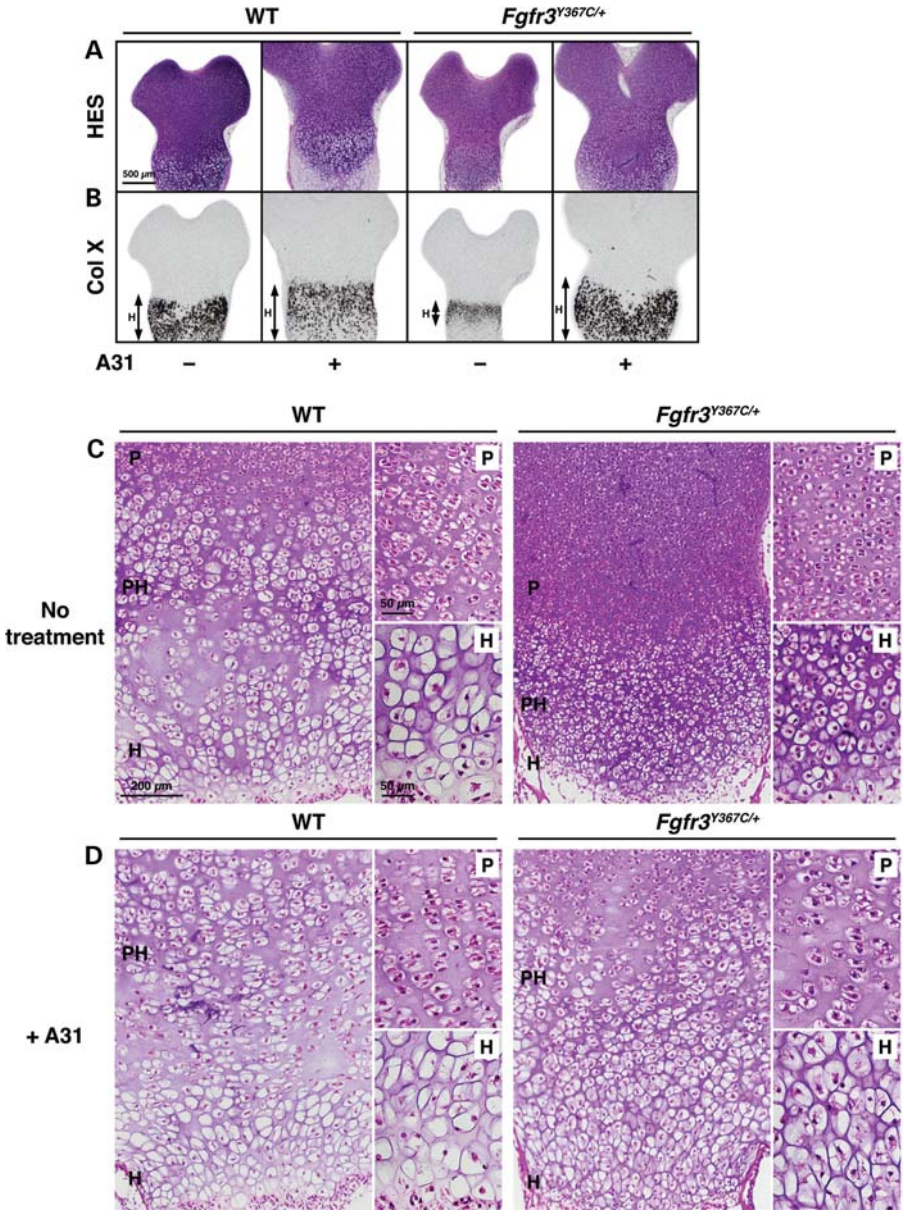

Figure 4. A31 modifies the size of the growth plate and chondrocyte morphology. (**A**) HES staining showing the reduced size of the *Fgfr3*$^{Y367C/+}$ growth plate. A31 induces an increase in the size of the growth plate of the *Fgfr3*$^{Y367C/+}$ mice. (**B**) *In situ* hybridization of type X collagen showing a markedly reduced hypertrophic zone (H) of *Fgfr3*$^{Y367C/+}$ growth plates compared with WT. A31 induces enhanced type X collagen expression in *Fgfr3*$^{Y367C/+}$ growth plates. (**C**) HES staining of WT and *Fgfr3*$^{Y367C/+}$ growth plates showing smaller mutant chondrocytes in proliferative (P) and hypertrophic (H) zones (high magnification). (**D**) HES staining showing the effect of A31 on chondrocyte phenotype. Cells appear more spherical in the proliferative (P) and hypertrophic zones (H).

p57 predominantly in late proliferative and PH chondrocytes. A31 reduced expression of p57 protein particularly in the PH zone and enabled PH chondrocytes to properly differentiate into H chondrocytes (Fig. 6E). We conclude that activated FGFR3 leads to over-expression of markers of proliferation (PCNA, KI67) and cell cycle regulators (cyclin D1 and p57) particularly in the PH zone. These data highlight the dysregulation of the cell cycle in this skeletal pathology.

DISCUSSION

ACH is the most common form of dwarfism in humans. Most evidence to date suggests that endochondral ossification is disrupted in FGFR3-related chondrodysplasias and *Fgfr3* mouse models (12–15). To understand the molecular physiopathology and to define the best approaches to treat the disease, we combined several approaches to understand the specific role of Fgfr3 during the endochondral ossification process.

Consistent with the abnormal bone growth due to FGFR3 mutations, inhibition of a constitutively active FGFR3 using a novel TKI, A31 (31) rescued bone growth, indicating that the inhibition of Fgfr3 was sufficient to overcome the growth defects of *Fgfr3*$^{Y367C/+}$ mice.

A31 inhibited constitutive FGFR3 phosphorylation in transfected cells and restored the size of dwarf femurs using an

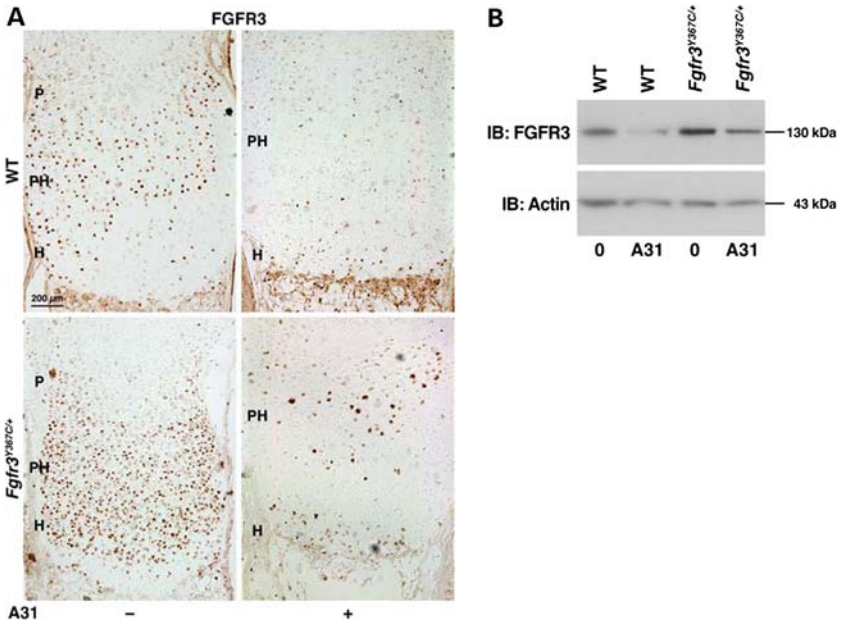

Figure 5. A31 decreases Fgfr3 overexpression in *Fgfr3*$^{Y367C/+}$ femurs. (**A**) Growth plates of WT and *Fgfr3*$^{Y367C/+}$ mice were subjected to immunohistochemical staining for Fgfr3. Mutant growth plates display an overexpression of Fgfr3 in PH and H zones, which is strongly decreased after A31 treatment. (**B**) Costal primary chondrocytes were examined by western-blot with anti-FGFR3. Fgfr3 protein level is higher in *Fgfr3*$^{Y367C/+}$ chondrocytes compared with WT. A31 reduced this overexpression.

ex vivo culture for embryonic femurs. The increase in length of the mutant femurs was 2.6 times more than that of WT. This approach allowed us to visualize more precisely the impact of the activated receptor on growth plate organization, gene expressions and chondrocyte morphology.

FGFR3 has been described both as a negative and a positive regulator of endochondral ossification (1–4), disrupting proliferation and terminal differentiation of growth plate chondrocytes, leading to inappropriate synthesis of extracellular matrix (36). However, the molecular mechanism underlying the harmonious transition from the proliferation to hypertrophic differentiation of chondrocytes remains an enigma. Human transcriptome data showed altered expression of genes downstream of mutated FGFR3, these genes were associated with many cellular processes, including cell proliferation, cell cycle and extracellular matrix structure and turnover (37).

Here, we focused our analysis on markers of proliferation and regulators of the cell cycle. As previously described in *Fgfr3* $^{K644E/+}$ mice, we observed a high number of PCNA- (12) and KI67-positive cells in *Fgfr3*$^{Y367C/+}$ fetal proliferative and PH zones, indicating a dysfunction of cell cycle regulation. The discrepancy in positive cell numbers between PCNA and KI67 may be due to immunolabeling of non-functional residual PCNA and/or involvement of PCNA in DNA repair (38).

In the cell cycle process, PCNA interacts with the cyclin-CDK complex to transduce positive or negative signals for progression to G1 or S phase (e.g. the binding of PCNA to the cyclin D-CDK complex is required for G1 progression, whereas cyclin E-CDK is required for progression to S phase) (39,40). In particular, Cyclin D1 has been shown to be required for normal proliferation of growth plate chondrocytes (41). Consistent with our previous human transcriptomic data (37), activated FGFR3 induced a significant overexpression of cyclin D1 in proliferative and PH chondrocytes of *Fgfr3*$^{Y367C/+}$ mice, thus promoting G1 phase presumably resulting in accelerated cell cycle progression. In accordance with our data, fibroblast growth factors or activated Fgfr3 induce cyclin D1 expression (42,43). Progression through the cell cycle is also controlled by CDKIs which negatively regulate the cell cycle (34). Here, we focused our attention on one CDKI, p57, which is known to inhibit the activity of all cyclin-CDK complexes involved in G1/S transition. The role of p57 has been studied in the p57$^{-/-}$ mouse model, in which the size of the resting and the proliferative zones of the growth plate were increased, whereas the number of hypertrophic chondrocytes was decreased (35,44). An important role for P57 was reported in the regulation of cell cycle exit and differentiation of chondrocytes (35). P57 has also been described as a mediator of proliferative actions of PTHrP in chondrocytes (45) and its transactivation by C/EBPb promotes the transition from proliferation to hypertrophic differentiation of chondrocytes (46). Here, activated Fgfr3 induced higher expression of p57 predominantly in late proliferative and PH chondrocytes. Taken together, our data suggest that even in a context of high cyclin D1 expression, P57 could shorten the cell cycle and induce premature chondrocyte differentiation. This hypothesis is in agreement with previous results of Minina *et al.* (47), showing that addition of FGF2 to bone explants induces an advanced onset of hypertrophic differentiation. FGFs also promote expression of genes associated with hypertrophic differentiation in rat chondrosarcoma cells (43).

The MAPK pathway has been identified downstream of FGFR3 activation and studies have demonstrated the impact of this pathway on the growth plate. In mice expressing a

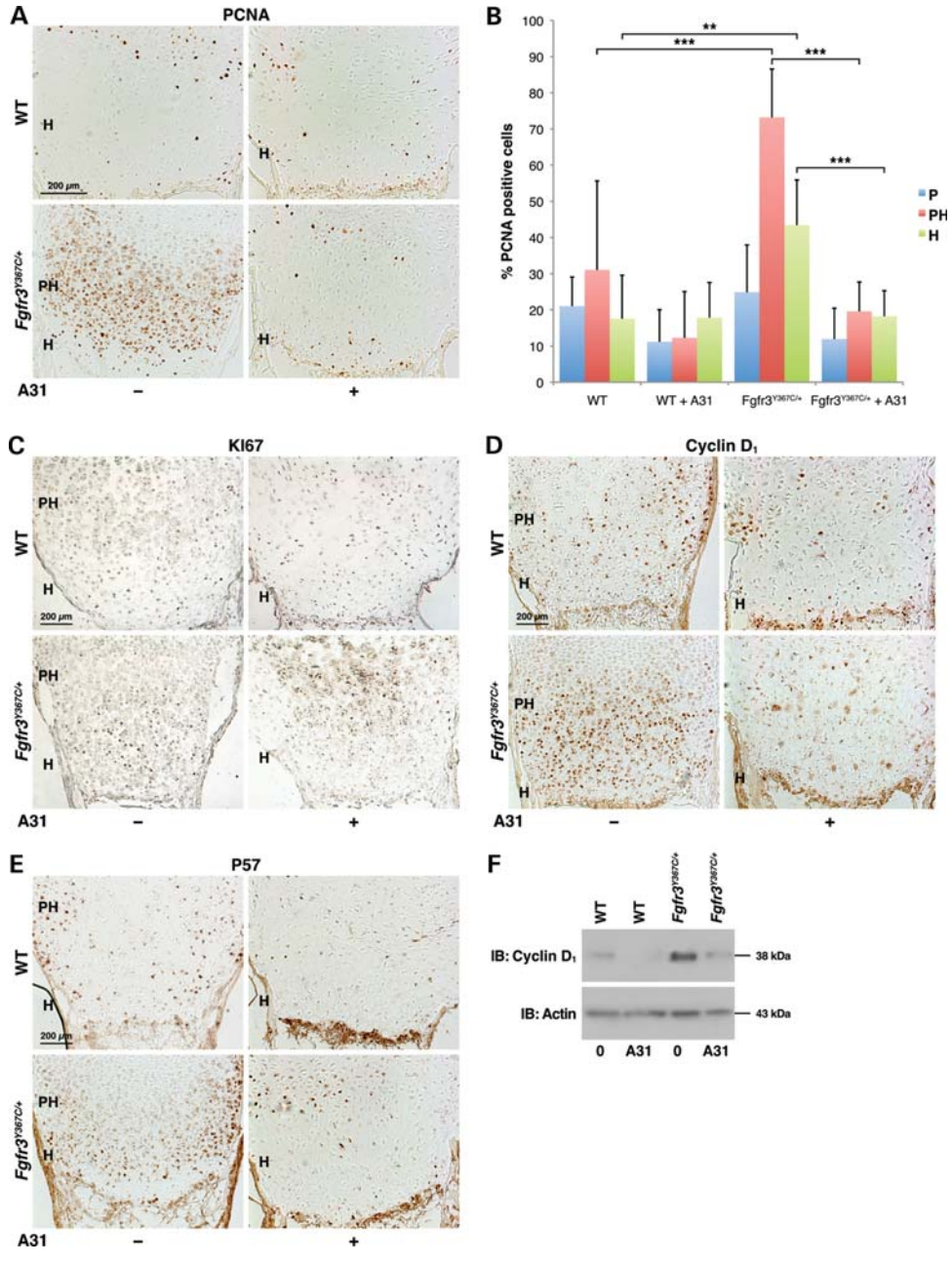

Figure 6. A31 reduces proliferation and cell cycle regulator expression in growth plates. (**A**) Immunohistochemical staining of growth plates with anti-PCNA antibodies showing an overexpression of PCNA in $Fgfr3^{Y367C/+}$mice. The expression of PCNA is reduced by A31. (**B**) Quantification of PCNA-positive cells in proliferative (P), PH and H zones showing a higher level of PCNA-positive cells in $Fgfr3^{Y367C/+}$ growth plates [73% (PH) and 43% (H), $^{**}P < 0{,}005$ versus WT] compared with WT [31% (PH) and 18% (H)]. A31 induces a strong decrease in PCNA expression in PH and H zones of $Fgfr3^{Y367C/+}$ growth plates [20% (PH) and 18% (H), $^{***}P < 10^{-4}$ versus untreated femurs]. The experiments were performed six times and three observers counted positive cells. % PCNA-positive cells are shown as mean ± SD. (**C**) Immunohistochemical staining of growth plates with anti-KI-67 antibodies showing high expression of KI67 in P and PH zones of the $Fgfr3^{Y367C/+}$ growth plate. The expression of KI67 was reduced by A31. (**D**) Immunohistochemical staining showing overexpression of cyclin D1 in the $Fgfr3^{Y367C/+}$ growth plate. A31 induces a decrease in cyclin D1 expression. (**F**) Immunoblot showing a higher cyclin D1 expression in costal primary $Fgfr3^{Y367C/+}$ chondrocytes compared with WT. A31 reduces the expression of cyclin D1 in $Fgfr3^{Y367C/+}$ chondrocytes. Actin is included as loading control. (**E**) Immunohistochemical staining showing a high level of expression of P57 in the $Fgfr3^{Y367C/+}$ growth plate compared with WT. A31 reduces P57 expression in the $Fgfr3^{Y367C/+}$ growth plate.

constitutively active mutant of MEK1, the MAPK pathway inhibits the hypertrophic differentiation (17). Indeed, sustained activation of the MAPK pathway (ERK1/ERK2) is necessary for the G1 to S progression and is associated with the accumulation of cyclin D1 in the G1 phase (48). These data suggest that a prolonged activation of ERK1 and ERK2 induces the expression of cyclin-dependent kinase inhibitors, which can also contribute to cell cycle exit.

The disorganization and the reduction in the growth plate in FGFR3-related chondrodysplasias may also result from the

disorganization of collagen fibrils, loss of matrix components and an altered gliding movement of chondrocytes (49). Here, we confirmed these abnormalities and restored the collagen type X expression after inhibition of the phosphorylation of the activated Fgfr3.

Collectively, these data allow us to conclude that key regulators of the cell cycle were disrupted in the growth plate of the *Fgfr3*$^{Y367C/+}$ mice. Activated FGFR3 disturbs the transition from the proliferative to the hypertrophic state. The duration of the cell cycle phase was shortened, inducing escape from the cell cycle and premature chondrocyte differentiation.

The TKI, A31, blocked FGFR3 kinase activity, restored bone growth dramatically, modulated the cell cycle (PCNA, KI67, cyclin D1, P67) and transformed PH chondrocytes into hypertrophic chondrocytes.

Kinase inhibitor drug discovery has progressed dramatically in the past decade and TKIs are being intensively pursued as new anticancer therapeutics (50). Here, we have successfully targeted FGFR3 kinase domains with a TKI in *Fgfr3*$^{Y367C/+}$ mice. These promising data provide a pre-clinical rationale for clinical investigation of TKIs in FGFR3-related chondrodysplasias.

MATERIALS AND METHODS

Chemical compound

A series of inhibitors was previously designed and synthesized as PD173074 [Park Davies (51)] analogues bearing various N-substituents. Of 27 analogues synthesized, A31 (refers to 19 g) was selected in the course of preliminary cellular assays for its ability to inhibit FGFR3 phosphorylation (31). This compound competes with ATP binding and can inhibit autophosphorylation of FGFR3, with an IC50 value of ~190 nM. As a control, we used the commercial FGFR TKI, PD 173074. TKIs were dissolved in DMSO at a concentration of 10 mM. The stock solution was stored at −20°C before use.

Computational analyses

The kinase domain structure of FGFR3 was predicted by homology modeling with the Esypred3D software (52) using a recent X-ray structure of the highly homologous FGFR1 protein (pdb code 3JS2) (33). We used AMBER software (53) according to a previously published protocol (54). We built A31 compound (31) using the Sybyl software package version 11.0 (SYBYL, Tripos Inc., St Louis, MO, USA). Two states of the asymmetric carbon (R, S) and two different protonation states of the neighboring amino moiety (neutral and +1) were considered. Four distinct chemical structures were obtained. Energy minimizations of these four A31 structures were performed (55). Docking calculations were carried out with version 4.2 of the program AutoDock (56). Kollman's united atomic charges were computed. A grid box of 23 × 20 × 33 Å was constructed in, respectively, the x-, y- and z-axes around the binding cavity. All ligand torsion angles were allowed to rotate during docking, leading to a complete flexibility. One hundred cycles of calculations of Lamarckian genetic algorithm were performed to complete the conformational search. One hundred resulting docking structures were clustered into conformation families according to a root mean square deviation lower than 2.0 Å. We selected the conformation, which presented the lowest docking free energy of binding in the most populated cluster.

Ex vivo experiments

Heterozygous *Fgfr3*$^{Y367C/+}$ mice ubiquitously expressing the Y367C mutation and exhibiting a severe dwarfism were used (14). Six sets of *ex vivo* experiments were performed. Femur embryos at day E16.5 from WT ($n = 6$) and *Fgfr3*$^{Y367C/+}$ ($n = 6$) mice were used and incubated for 5 days in Dulbecco's modified eagle medium (DMEM) with antibiotics and 0.2% bovine serum albumin (BSA) (Sigma) supplemented with A31 or PD173074 (as control) at a concentration of 2 mM. Right femur was cultured in the supplemented medium and compared with the left one cultured in the control medium. Rib cage from E16.5 WT and *Fgfr3*$^{Y367C/+}$ mice embryos were isolated and stripped of all soft tissues. Primary chondrocytes were obtained from rib cages. The ribs were incubated in a pronase solution (Roche; 2 mg/ml) followed by a digestion in collagenase A (Roche; 3 mg/ml) at 37°C. Isolated chondrocytes were plated out at a density of 2.10^5 cells in six-well plates containing DMEM supplemented with 10% fetal calf serum and antibiotics, and were allowed to reach subconfluency. Cultures were supplemented with A31 or PD173074 (as control) at a concentration of 2 mM. Cells were treated with A31 (2 mM) and PD173074 (as control) in serum-free DMEM supplemented with 0.2% BSA and harvested after 24 h. To establish the effect of the inhibitors, the right femur was cultured in the supplemented medium and compared with the left one cultured in the control medium The bone length was measured at the beginning (before treatment) and at the end of time course. Each experiment was repeated at least three times.

The genotype of WT, *Fgfr3*$^{Y367C/+}$ and *Fgfr3*$^{-/-}$ mice was determined by polymerase chain reaction of tail DNA as previously described (14). All experimental procedures and protocols were approved by the Animal Care and Use Committee.

Histological, *in situ* hybridization and immunohistochemical analyses

Limb explants were fixed after culture in 4% paraformaldehyde at 4°C, and placed in a staining solution for 45–60 min (0.05% Alizarin Red, 0.015% Alcian Blue, 5% acetic acid in 70% ethanol) or embedded in paraffin. Serial sections of 5\xEF\x80 mm were stained with hematoxylin–eosin using standard protocols for histological analysis or were subjected to *in situ* hybridization or immunohistochemical staining. *In situ* hybridization using [S^{35}]-UTP labeled antisense riboprobes for collagen X was carried out as previously described (26). Sections were counterstained with hematoxylin. For immunohistochemistry, sections were stained with antibodies specific to FGFR3 (1:250 dilution; Sigma), anti-PCNA (1:1000 dilution; Abcam), anti KI67 (1:300; Abcam), anti-cyclin D1 (1:80 dilution; Santa Cruz) and anti p57 (1:100 dilution; Santa Cruz) using the Dako Envision kit. Images were captured with an Olympus PD70-IX2-UCB microscope.

Quantification of PCNA expression

Three observers counted PCNA-positive and -negative chondrocytes in proliferative (P), PH and hypertrophic (H) zones of the growth plate. Student's *t*-test was used to compare treated (A31) and untreated femurs. Imagine software cellSens (Olympus) was used for counting cells. We considered a P-value < 0.05 significant.

Immunoprecipiation, immunoblotting and immunocytochemistry experiments

Human embryonic kidney (HEK) cells and human chondrocyte lines (32) were transfected transiently with FGFR3 human constructs ($FGFR3^{Y373C}$, $FGFR3^{K650M}$, $FGFR3^{K650E}$) (28) using Fugene 6 (Roche). A31 (31) or PD173074 (Parke Davies) was added at a concentration of 2 mM overnight. Transfected cells were lysed in radio-immunoprecipitation assay buffer (50 mM Tris–HCl pH 7.6, 150 mM NaCl, 0.5% NP40, 0.25% sodium deoxycholate, supplemented with protease and phosphatase inhibitors). Immunoprecipitation was performed by incubating 3 ml rabbit anti-FGFR3 (Sigma)/500 mg protein with protein A-agarose (Roche). Immunoprecipitated proteins were subjected to sodium dodecyl sulfate (SDS)–polyacrylamide gel electrophoresis on NuPAGE 4–12% bis–tris acrylamide gels (Invitrogen). Immunoprecipitated proteins were subjected to SDS–polyacrylamide gels electrophoresis on NuPAGE 4–12% bis–tris acrylamide gels (Invitrogen). Blots were hybridized overnight at 4°C with anti-FGFR3 polyclonal antibody (1:1,000 dilution; Sigma), or anti-phosphotyrosine monoclonal antibody (1:400 dilution; Cell Signaling). Lysates of primary murine chondrocytes (E16.5) were subjected to SDS–polyacrylamide gel electrophoresis and were hybridized overnight at 4°C with anti-cyclin D1 monoclonal antibody (1:100 dilution; Santa Cruz). A secondary antibody, anti-rabbit or anti-mouse coupled to peroxidase, was used at a dilution of 1:10 000 (Amersham). Bound proteins were detected by chemiluminescence (ECL, Amersham). The blots were rehybridized with an anti-pan-actin antibody for quantification (Millipore).

For immunocytochemistry, we used the following primary antibodies: anti-FGFR3 antibodies (1:400 dilution; Sigma), anti-phosphotyrosine antibodies (1:200 dilution; Cell Signaling) and secondary antibodies Alexa Fluor®488 goat anti-rabbit and Alexa Fluor®568 goat anti-mouse (1:400 dilution; Molecular Probes). Cells were covered with Faramount Aquaeous Mounting Medium (Dako) and analyzed using an Olympus PD70-IX2-UCB microscope.

Proliferation studies

NIH-3T3 clones stably expressing $FGFR3^{+/+}$ (WT) and $FGFR3^{Y373C}$, $FGFR3^{K650M}$ (human constructs) were used. The stable clones were selected with G418. NIH-3T3 clones were incubated for 8 h in 10% newborn calf serum DMEM supplemented or not with A31 (2 mM). [^{3}H] thymidine was added at a concentration of 10 mCi/ml and incubated for 16 h. The cells were harvested on glass fiber filter paper and assayed for radioactivity by liquid scintillation counting. We used Top Count Microplates scintillation counter (Perkin Elmer).

SUPPLEMENTARY MATERIAL

Supplementary Material is available at *HMG* online.

ACKNOWLEDGEMENTS

We thank Chantal Esculpavit and Gérard Pivert for their technical assistance and Eric Le Gall for the art work.

Conflict of Interest statement. None declared.

FUNDING

Part of this work was supported by the EuroGrow (FP6-STREP- LSHM-CT-2007-037471) and the Albert de Costa association.

REFERENCES

1. Liu, Z., Lavine, K.J., Hung, I.H. and Ornitz, D.M. (2007) FGF18 is required for early chondrocyte proliferation, hypertrophy and vascular invasion of the growth plate. *Dev. Biol.*, **302**, 80–91.
2. Pannier, S., Mugniery, E., Jonquoy, A., Benoist-Lasselin, C., Odent, T., Jais, J.P., Munnich, A. and Legeai-Mallet, L. (2010) Delayed bone age due to a dual effect of FGFR3 mutation in Achondroplasia. *Bone*, **47**, 905–915.
3. Colvin, J.S., Bohne, B.A., Harding, G.W., McEwen, D.G. and Ornitz, D.M. (1996) Skeletal overgrowth and deafness in mice lacking fibroblast growth factor receptor 3. *Nat. Genet.*, **12**, 390–397.
4. Deng, C., Wynshaw-Boris, A., Zhou, F., Kuo, A. and Leder, P. (1996) Fibroblast growth factor receptor 3 is a negative regulator of bone growth. *Cell*, **84**, 911–921.
5. Rousseau, F., Bonaventure, J., Legeai-Mallet, L., Pelet, A., Rozet, J.M., Maroteaux, P., Le Merrer, M. and Munnich, A. (1994) Mutations in the gene encoding fibroblast growth factor receptor-3 in achondroplasia. *Nature*, **371**, 252–254.
6. Shiang, R., Thompson, L.M., Zhu, Y.Z., Church, D.M., Fielder, T.J., Bocian, M., Winokur, S.T. and Wasmuth, J.J. (1994) Mutations in the transmembrane domain of FGFR3 cause the most common genetic form of dwarfism, achondroplasia. *Cell*, **78**, 335–342.
7. Bellus, G.A., McIntosh, I., Smith, E.A., Aylsworth, A.S., Kaitila, I., Horton, W.A., Greenhaw, G.A., Hecht, J.T. and Francomano, C.A. (1995) A recurrent mutation in the tyrosine kinase domain of fibroblast growth factor receptor 3 causes hypochondroplasia. *Nat. Genet.*, **10**, 357–359.
8. Rousseau, F., Bonaventure, J., Legeai-Mallet, L., Schmidt, H., Weissenbach, J., Maroteaux, P., Munnich, A. and Le Merrer, M. (1996) Clinical and genetic heterogeneity of hypochondroplasia. *J. Med. Genet.*, **33**, 749–752.
9. Tavormina, P.L., Shiang, R., Thompson, L.M., Zhu, Y.Z., Wilkin, D.J., Lachman, R.S., Wilcox, W.R., Rimoin, D.L., Cohn, D.H. and Wasmuth, J.J. (1995) Thanatophoric dysplasia (types I and II) caused by distinct mutations in fibroblast growth factor receptor 3. *Nat. Genet.*, **9**, 321–328.
10. Rousseau, F., Saugier, P., Le Merrer, M., Munnich, A., Delezoide, A.L., Maroteaux, P., Bonaventure, J., Narcy, F. and Sanak, M. (1995) Stop codon FGFR3 mutations in thanatophoric dwarfism type 1. *Nat. Genet.*, **10**, 11–12.
11. Rousseau, F., el Ghouzzi, V., Delezoide, A.L., Legeai-Mallet, L., Le Merrer, M., Munnich, A. and Bonaventure, J. (1996) Missense FGFR3 mutations create cysteine residues in thanatophoric dwarfism type I (TD1). *Hum. Mol. Genet.*, **5**, 509–512.
12. Iwata, T., Chen, L., Li, C., Ovchinnikov, D.A., Behringer, R.R., Francomano, C.A. and Deng, C.X. (2000) A neonatal lethal mutation in FGFR3 uncouples proliferation and differentiation of growth plate chondrocytes in embryos. *Hum. Mol. Genet.*, **9**, 1603–1613.

13. Naski, M.C., Colvin, J.S., Coffin, J.D. and Ornitz, D.M. (1998) Repression of hedgehog signaling and BMP4 expression in growth plate cartilage by fibroblast growth factor receptor 3. *Development*, **125**, 4977–4988.
14. Pannier, S., Couloigner, V., Messaddeq, N., Elmaleh-Berges, M., Munnich, A., Romand, R. and Legeai-Mallet, L. (2009) Activating Fgfr3 Y367C mutation causes hearing loss and inner ear defect in a mouse model of chondrodysplasia. *Biochim. Biophys. Acta*, **1792**, 140–147.
15. Segev, O., Chumakov, I., Nevo, Z., Givol, D., Madar-Shapiro, L., Sheinin, Y., Weinreb, M. and Yayon, A. (2000) Restrained chondrocyte proliferation and maturation with abnormal growth plate vascularization and ossification in human FGFR-3(G380R) transgenic mice. *Hum. Mol. Genet.*, **9**, 249–258.
16. Legeai-Mallet, L., Benoist-Lasselin, C., Delezoide, A.L., Munnich, A. and Bonaventure, J. (1998) Fibroblast growth factor receptor 3 mutations promote apoptosis but do not alter chondrocyte proliferation in thanatophoric dysplasia. *J. Biol. Chem.*, **273**, 13007–13014.
17. Murakami, S., Balmes, G., McKinney, S., Zhang, Z., Givol, D. and de Crombrugghe, B. (2004) Constitutive activation of MEK1 in chondrocytes causes Stat1-independent achondroplasia-like dwarfism and rescues the Fgfr3-deficient mouse phenotype. *Genes Dev.*, **18**, 290–305.
18. Matsushita, T., Wilcox, W.R., Chan, Y.Y., Kawanami, A., Bukulmez, H., Balmes, G., Krejci, P., Mekikian, P.B., Otani, K., Yamaura, I. *et al.* (2009) FGFR3 promotes synchondrosis closure and fusion of ossification centers through the MAPK pathway. *Hum. Mol. Genet.*, **18**, 227–240.
19. Krejci, P., Salazar, L., Goodridge, H.S., Kashiwada, T.A., Schibler, M.J., Jelinkova, P., Thompson, L.M. and Wilcox, W.R. (2008) STAT1 and STAT3 do not participate in FGF-mediated growth arrest in chondrocytes. *J. Cell Sci.*, **121**, 272–281.
20. Su, W.C., Kitagawa, M., Xue, N., Xie, B., Garofalo, S., Cho, J., Deng, C., Horton, W.A. and Fu, X.Y. (1997) Activation of Stat1 by mutant fibroblast growth-factor receptor in thanatophoric dysplasia type II dwarfism. *Nature*, **386**, 288–292.
21. Legeai-Mallet, L., Benoist-Lasselin, C., Munnich, A. and Bonaventure, J. (2004) Overexpression of FGFR3, Stat1, Stat5 and p21Cip1 correlates with phenotypic severity and defective chondrocyte differentiation in FGFR3-related chondrodysplasias. *Bone*, **34**, 26–36.
22. Li, C., Chen, L., Iwata, T., Kitagawa, M., Fu, X.Y. and Deng, C.X. (1999) A Lys644Glu substitution in fibroblast growth factor receptor 3 (FGFR3) causes dwarfism in mice by activation of STATs and ink4 cell cycle inhibitors. *Hum. Mol. Genet.*, **8**, 35–44.
23. Ulici, V., Hoenselaar, K.D., Agoston, H., McErlain, D.D., Umoh, J., Chakrabarti, S., Holdsworth, D.W. and Beier, F. (2009) The role of Akt1 in terminal stages of endochondral bone formation: angiogenesis and ossification. *Bone*, **45**, 1133–1145.
24. Monsonego-Ornan, E., Adar, R., Feferman, T., Segev, O. and Yayon, A. (2000) The transmembrane mutation G380R in fibroblast growth factor receptor 3 uncouples ligand-mediated receptor activation from down-regulation. *Mol. Cell Biol.*, **20**, 516–522.
25. Monsonego-Ornan, E., Adar, R., Rom, E. and Yayon, A. (2002) FGF receptors ubiquitylation: dependence on tyrosine kinase activity and role in downregulation. *FEBS Lett.*, **528**, 83–89.
26. Delezoide, A.L., Lasselin-Benoist, C., Legeai-Mallet, L., Brice, P., Senee, V., Yayon, A., Munnich, A., Vekemans, M. and Bonaventure, J. (1997) Abnormal FGFR 3 expression in cartilage of thanatophoric dysplasia fetuses. *Hum. Mol. Genet.*, **6**, 1899–1906.
27. Cho, J.Y., Guo, C., Torello, M., Lunstrum, G.P., Iwata, T., Deng, C. and Horton, W.A. (2004) Defective lysosomal targeting of activated fibroblast growth factor receptor 3 in achondroplasia. *Proc. Natl Acad. Sci. USA*, **101**, 609–614.
28. Gibbs, L. and Legeai-Mallet, L. (2007) FGFR3 intracellular mutations induce tyrosine phosphorylation in the Golgi and defective glycosylation. *Biochim. Biophys. Acta*, **1773**, 502–512.
29. Bonaventure, J., Horne, W.C. and Baron, R. (2007) The localization of FGFR3 mutations causing thanatophoric dysplasia type I differentially affects phosphorylation, processing and ubiquitylation of the receptor. *FEBS J.*, **274**, 3078–3093.
30. Laederich, M.B. and Horton, W.A. (2010) Achondroplasia: pathogenesis and implications for future treatment. *Curr. Opin. Pediatr.*, **22**, 516–523.
31. Le Corre, L., Girard, A.L., Aubertin, J., Radvanyi, F., Benoist-Lasselin, C., Jonquoy, A., Mugniery, E., Legeai-Mallet, L., Busca, P. and Le Merrer, Y. (2010) Synthesis and biological evaluation of a triazole-based library of pyrido[2,3-d]pyrimidines as FGFR3 tyrosine kinase inhibitors. *Org. Biomol. Chem.*, **8**, 2164–2173.
32. Benoist-Lasselin, C., Gibbs, L., Heuertz, S., Odent, T., Munnich, A. and Legeai-Mallet, L. (2007) Human immortalized chondrocytes carrying heterozygous FGFR3 mutations: an *in vitro* model to study chondrodysplasias. *FEBS Lett.*, **581**, 2593–2598.
33. Ravindranathan, K.P., Mandiyan, V., Ekkati, A.R., Bae, J.H., Schlessinger, J. and Jorgensen, W.L. (2010) Discovery of novel fibroblast growth factor receptor 1 kinase inhibitors by structure-based virtual screening. *J. Med. Chem.*, **53**, 1662–1672.
34. LuValle, P. and Beier, F. (2000) Cell cycle control in growth plate chondrocytes. *Front. Biosci.*, **5**, D493–D503.
35. Yan, Y., Frisen, J., Lee, M.H., Massague, J. and Barbacid, M. (1997) Ablation of the CDK inhibitor p57Kip2 results in increased apoptosis and delayed differentiation during mouse development. *Genes Dev.*, **11**, 973–983.
36. Horton, W.A. and Degnin, C.R. (2009) FGFs in endochondral skeletal development. *Trends Endocrinol. Metab.*, **20**, 341–348.
37. Schibler, L., Gibbs, L., Benoist-Lasselin, C., Decraene, C., Martinovic, J., Loget, P., Delezoide, A.L., Gonzales, M., Munnich, A., Jais, J.P. *et al.* (2009) New insight on FGFR3-related chondrodysplasias molecular physiopathology revealed by human chondrocyte gene expression profiling. *PLoS ONE*, **4**, e7633.
38. Blankenship, T.N. and King, B.F. (1994) Developmental expression of Ki-67 antigen and proliferating cell nuclear antigen in macaque placentas. *Dev. Dyn.*, **201**, 324–333.
39. Gulbis, J.M., Kelman, Z., Hurwitz, J., O'Donnell, M. and Kuriyan, J. (1996) Structure of the C-terminal region of p21(WAF1/CIP1) complexed with human PCNA. *Cell*, **87**, 297–306.
40. Xiong, Y., Zhang, H. and Beach, D. (1992) D type cyclins associate with multiple protein kinases and the DNA replication and repair factor PCNA. *Cell*, **71**, 505–514.
41. Beier, F., Ali, Z., Mok, D., Taylor, A.C., Leask, T., Albanese, C., Pestell, R.G. and LuValle, P. (2001) TGFbeta and PTHrP control chondrocyte proliferation by activating cyclin D1 expression. *Mol. Biol. Cell*, **12**, 3852–3863.
42. Rozenblatt-Rosen, O., Mosonego-Ornan, E., Sadot, E., Madar-Shapiro, L., Sheinin, Y., Ginsberg, D. and Yayon, A. (2002) Induction of chondrocyte growth arrest by FGF: transcriptional and cytoskeletal alterations. *J. Cell Sci.*, **115**, 553–562.
43. Dailey, L., Laplantine, E., Priore, R. and Basilico, C. (2003) A network of transcriptional and signaling events is activated by FGF to induce chondrocyte growth arrest and differentiation. *J. Cell Biol.*, **161**, 1053–1066.
44. Zhang, P., Liegeois, N.J., Wong, C., Finegold, M., Hou, H., Thompson, J.C., Silverman, A., Harper, J.W., DePinho, R.A. and Elledge, S.J. (1997) Altered cell differentiation and proliferation in mice lacking p57KIP2 indicates a role in Beckwith-Wiedemann syndrome. *Nature*, **387**, 151–158.
45. MacLean, H.E., Guo, J., Knight, M.C., Zhang, P., Cobrinik, D. and Kronenberg, H.M. (2004) The cyclin-dependent kinase inhibitor p57(Kip2) mediates proliferative actions of PTHrP in chondrocytes. *J. Clin. Invest.*, **113**, 1334–1343.
46. Hirata, M., Kugimiya, F., Fukai, A., Ohba, S., Kawamura, N., Ogasawara, T., Kawasaki, Y., Saito, T., Yano, F., Ikeda, T. *et al.* (2009) C/EBPbeta promotes transition from proliferation to hypertrophic differentiation of chondrocytes through transactivation of p57. *PLoS ONE*, **4**, e4543.
47. Minina, E., Kreschel, C., Naski, M.C., Ornitz, D.M. and Vortkamp, A. (2002) Interaction of FGF, Ihh/Pthlh, and BMP signaling integrates chondrocyte proliferation and hypertrophic differentiation. *Dev. Cell*, **3**, 439–449.
48. Meloche, S. and Pouyssegur, J. (2007) The ERK1/2 mitogen-activated protein kinase pathway as a master regulator of the G1- to S-phase transition. *Oncogene*, **26**, 3227–3239.
49. Morales, T.I. (2007) Chondrocyte moves: clever strategies? *Osteoarthritis Cartilage*, **15**, 861–871.
50. Zhang, J., Yang, P.L. and Gray, N.S. (2009) Targeting cancer with small molecule kinase inhibitors. *Nat. Rev. Cancer*, **9**, 28–39.
51. Miyake, M., Ishii, M., Koyama, N., Kawashima, K., Kodama, T., Anai, S., Fujimoto, K., Hirao, Y. and Sugano, K. (2010) 1-tert-butyl-3-[6-(3,5-dimethoxy-phenyl)-2-(4-diethylamino-butylamino)-pyr ido[2,3-d]pyrimidin-7-yl]-urea (PD173074), a selective tyrosine kinase inhibitor of fibroblast growth factor receptor-3 (FGFR3), inhibits cell proliferation of bladder cancer carrying the FGFR3 gene mutation along with up-regulation of p27/Kip1 and G1/G0 arrest. *J. Pharmacol. Exp. Ther.*, **332**, 795–802.

52. Lambert, C., Leonard, N., De Bolle, X. and Deperieux, E. (2002) EsyPred3D: prediction of proteins 3D structures. *Bioinformatics*, **18**, 1250–1256.
53. Case, D.A., Darden, T.A., Cheatham, T.E., Simmerling, C.L., Wang, J., Duke, R.E., Luo, R., Merz, K.M., Pearlman, D.A., Crowley, M. *et al.* (2006) Amber. San Francisco: University of California. http://ambermd.org/.
54. Luo, Y., Barbault, F., Gourmala, C., Zhang, Y., Maurel, F., Yongzhou, H. and Fan, B.T. (2008) Cellular interaction through LewisX cluster: theoretical studies. *J. Mol. Model*, **14**, 901–910.
55. Hu, R., Barbault, F., Delamar, M. and Zhang, R. (2009) Receptor- and ligand-based 3D-QSAR study for a series of non-nucleoside HIV-1 reverse transcriptase inhibitors. *Bioorg. Med. Chem.*, **17**, 2400–2409.
56. Morris, G.M., Goodsell, D.S., Halliday, R.S., Huey, R., Hart, W.E., Belew, R.K. and Olson, A.J. (1998) Automated docking using a Lamarckian genetic algorithm and an empirical binding free energy function. *J. Comput. Chem.*, **19**, 1639–1662.